Structural biochemistry of the pentraxins

Noone, D.P.

7 A platform for the interrogation of membrane bound PTX3

Dylan P. Noone[1], Tom A. W. Schoufour[1], Ruud H. Wijdeven[1], Douwe J. Dijkstra[2], Teun T. van der Klugt[1], Leendert A. Trouw[2], Jacques Neefjes[1] and Thomas H. Sharp[1,*]

[1]Department of Cell and Chemical Biology, Leiden University Medical Center, 2300 RC Leiden, The Netherlands

[2]Department of Immunology, Leiden University Medical Center, 2333 ZA, Leiden, The Netherlands

*To whom correspondence should be addressed: t.sharp@lumc.nl

Abstract

The pentraxins are a family of soluble pattern recognition receptors (PRRs) with roles in pathogen recognition and silent clearance of apoptotic cells. The pentraxin family is divided into the short and long pentraxins, the latter containing additional N-terminal domains of which PTX3 is the prototypical member. It is known that PTX3 forms multimers that activate the immune system by binding to the C1 complex. However, the recent publication of a high-resolution structure of PTX3 revealed a protein architecture that is different to that of the other pentraxins, suggesting that PTX3 may use different structural arrangements when binding C1. Additionally, PTX3 contains diverse ligand binding sites scattered across the protein, suggesting that it may also form different structural constellations when binding to different ligands. To interrogate this, we produced liposome cell mimetics that were decorated with PTX3, which was confirmed by Western blot and electron microscopy (EM). However, whilst PTX3 could bind the C1 complex in enzyme-linked immunosorbent assay (ELISA), liposome bound PTX3 failed to induce complement activation via the C1 complex, possibly due to the artificial nature of the interaction between PTX3 and the lipid surface. To remedy this, we sought a native biologically relevant ligand using a CRISPR based genome wide screen, which revealed a novel transmembrane ligand CLEC1B that could be used in further studies. Further development of this approach would enable the imaging of PTX3 bound to a range of other ligands, such as influenza hemagglutinin or CD44, potentially revealing structural and functional insights into diverse conditions ranging from viral infection to cancer.

Introduction

The immune system protects the body from pathogens and damage via recognition of motifs associated with danger(4), which are detected by an arsenal of pattern recognition receptors (PRRs)(224, 225). Recognition of motifs by PRRs can activate the complement system, which is classically thought of as part of the innate immune system(7). The pentraxin family is a group of soluble PRRs that comprise the short and long pentraxins, exemplified by C-reactive protein (CRP)(13) and PTX3(39), respectively, with the long pentraxins containing an extra N-terminal region(39). The long pentraxin PTX3 is locally expressed at sites of inflammation in a wide range of tissues, including the respiratory tract, muscles, and female reproductive tissues, reflecting its role in pathogen recognition(51), tissue repair(83), and as a structural component of the extracellular matrix (ECM)(200). The unique N-terminal domain of PTX3 has been hypothesised to introduce additional functions via an expanded ligand binding repertoire. PTXs also has a different protein architecture compared to the pentameric ring structures of the short pentraxins CRP(34) and SAP(37), containing a octameric pentraxin core flanked by two tetrameric coiled coil N-terminal domains(36). In order to bind and activate C1, PTX3 forms higher order oligomers(137, 140), though the exact structural configuration of this initiation complex is unknown. Other complement activators such as IgG1 and IgG3 circulate as inactive monomers that form higher order oligomers when bound to membrane antigens, in order to bind and activate the C1 complex(8, 138). Recently, as seen in ***chapter 3***,

the small pentraxin CRP has been observed to circulate as inactive complexes which assemble laterally into higher order structures upon membrane binding. However, as PTX3 is roughly twice the size of CRP and has a completely different protein architecture(36), PTX3 may use different structural arrangements when binding to and activating C1. Moreover, PTX3 can bind to complement regulatory proteins, such as factor-H, to dampen complement activation(44, 210), biasing it towards silent clearance of cells(61). As such, investigating how membrane-bound PTX3 can bind to ligands such as C1 and factor-H may reveal how PRRs can switch between silent clearance of cellular debris and inflammatory processes such as the lysis of pathogens. This may also provide valuable insights into pathologies such as cancer, where PTX3 based complement activation can become dysregulated(31). Previously, IgG-1(8), IgM(9), IgG-3(138) and CRP (***chapter 3***) have been imaged on cell mimetic liposomes via cryoelectron tomography (cryoET) to produce *in situ* structures of these complexes bound to C1. This chapter represents the first steps into developing a similar system for imaging membrane-bound PTX3 bound to biologically relevant ligands. To achieve this, we linked PTX3 to liposomes containing Ni-NTA conjugated lipids, via purification tags present on the recombinant PTX3 preparation used in this study. PTX3 co-precipitated with liposomes after separation from the liquid phase and showed an additional band when co-incubated with normal human serum (NHS), suggesting interaction with a ligand found in NHS. Binding of PTX3 to liposomes was confirmed via electron microscopy (EM) and cryoelectron microscopy (cryoEM), showing that PTX3 bound to the liposomes via the flexible N-terminal domains, consistent with interactions between the His_6-tag and the Ni-NTA conjugated lipids. PTX3 could bind to C1, but did not result in complement activation, possibly relating to aspects of the experimental setup, such as the artificial nature of the interaction between the liposome and PTX3. To circumvent this issue, native membrane ligands may have to be used in the future. As such, a CRISPR based genome wide screen for transmembrane ligands was utilised, which resulted in the detection of a novel interactor, CLEC1B. Taken together, this study represents the first tentative steps towards interrogating membrane bound PTX3 multimers and their interaction with ligands such as the C1 complex.

Results and Discussions

Complement activation often requires membrane-associated ligands or antigens being bound by inactive monomers of complement activator proteins such as IgG, which results in the formation of higher order oligomers that can activate the C1 complex (8, 9, 138). In keeping with this mechanism, PTX3 is also known to activate complement via the formation of higher-order multimers(140), as well as interacting with complement regulatory proteins to inhibit subsequent activation (31, 44, 210). However, the exact structural arrangement of PTX3 in this process is unknown and may differ greatly to that of CRP, IgG or IgM, due to the unique size and architecture of PTX3 (36). To image PTX3 multimers binding to ligands such as C1 on lipid membranes, recombinant PTX3 was linked to liposomes via an N-terminal His_6-tag interacting with Ni-NTA conjugated lipids (5%, mol%), in a similar manner to what has been previously reported for the synthetic reconstitution of membrane-bound HIV-1 trimers(226).

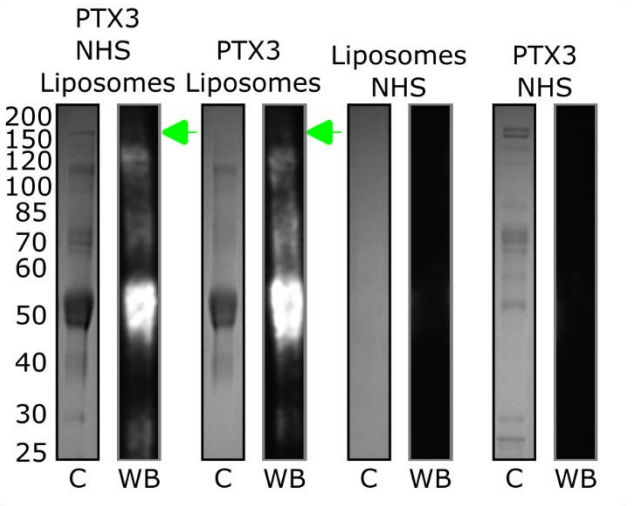

Figure 1: PTX3 binds to Ni-NTA decorated liposomes. *Coomassie stained 4-12% polyacrylamide gels (C) and Western Blot (WB) for His_6-tagged proteins. (Left to right) Resuspensions of the membrane bound fraction of PTX3 incubated with liposomes (DMPC:40, Chol:50, DMPG:5, DGS-Ni-NTA:5, mol%) and normal human serum (NHS), PTX3 with liposomes, liposomes with NHS, and PTX3 with NHS. Molecular weights are indicated on the lefthand side. PTX3 was added at 500 nM and NHS at 10%.*

Incubation of PTX3, NHS (10%) and liposomes lead to co-precipitation of protein with the liposomal pellet after centrifugation (**Fig. 1**). The majority of this could be attributed to PTX3 as detected via Western Blotting (**Fig. 1**) and exhibited a pattern similar to that which has been previously reported(36); namely two monomeric species, probably representing different glycosylation states(36, 50), combined with the presence of DTT resistant higher order oligomers (36, 40). In the absence of NHS, protein also co-sedimented with the liposomes, showing that PTX3 binds to the liposomes independently of factors from NHS. However, a band at around 150 kDa was absent (arrow in **Fig**. 1). As this band was not attributed to PTX3 via Western Blot, this may suggest that PTX3 binds an additional serum-based factor, possibly representing elements of the complement system(31, 137, 140, 227, 228) or complement regulatory proteins(31, 44, 210). Liposomes did not appear to co-sediment with proteins from NHS independently of PTX3, as no protein could be detected after incubation with NHS (**Fig. 1**). This indicates that co-incubation of PTX3 with liposomes is responsible for the detection of protein deposited on or bound to liposomes. However, PTX3 incubated with NHS in the absence of liposomes did appear to lead to the co-precipitation of some protein, though this did not appear to be PTX3 (**Fig. 1**). This could be the result of PTX3-induced fluid phase activation of the complement cascade, causing large aggregates of deposited complement proteins such as C4b to form and be pelleted by centrifugation. In turn, this may suggest that PTX3 forms higher order oligomers in liquid phase, in keeping with previous reports of higher order oligomers detected via size exclusion chromatography (SEC)(41). Taken together, this suggests that PTX3 can be linked to Ni-NTA-conjugated liposomes, and that it may bind to an unidentified serum based factor.

In the past, electron microscopy (EM) has proved useful in interrogating interactions between immunological proteins and their ligands, such as between IgG or IgM with C1(8, 9) and could therefore be applied to PTX3 to reveal insights as to how PTX3 activates the immune system. As shown above, PTX3 binds to Ni-NTA conjugated lipids, probably via the His_6-tag on the N-terminal of the protein (**Fig. 2A**). As such, liposomes incubated with PTX3 were imaged via EM, showing that this led to the decoration of liposome with protein consistent with PTX3; specifically, complexes with an electron dense core flanked by long flexible regions protruding out either side, reflecting the octameric pentraxin domain core and long flexible N-terminal domains(36) (**Fig. 2B**). This was also seen using cryoEM, with the N-terminal domains appearing to be the region of interaction between the liposomes and protein, consistent with

His_6-tag Ni-NTA interactions mediating association with the liposomes (**Fig. 2C**). However, under both conditions there appeared to be no formation of higher order oligomers as previously seen for the short pentraxin CRP (***chapter 3***).

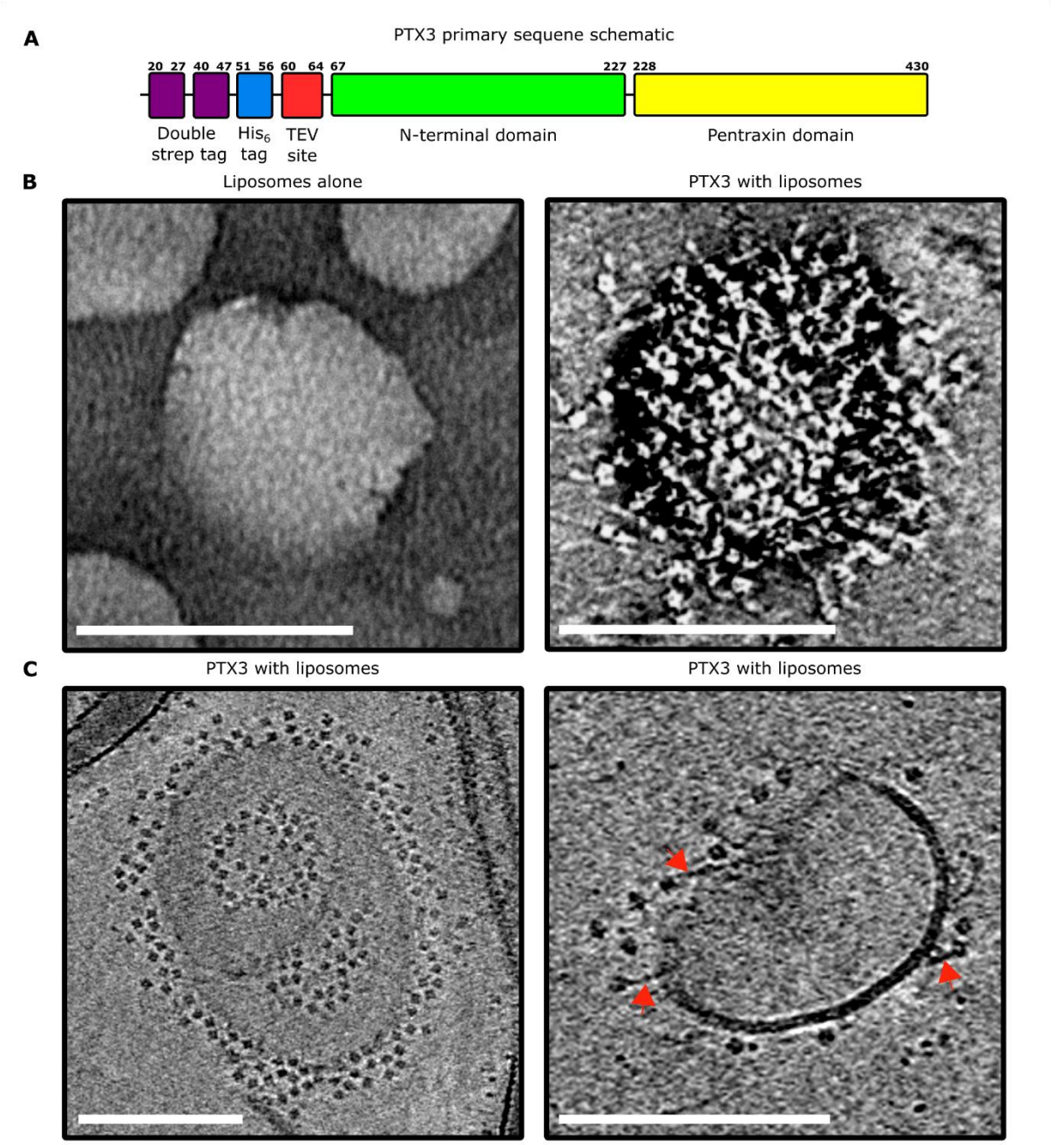

Figure 2: PTX3 binds to liposomes via N-terminal domains. *(**A**) Schematic of the primary sequence and domain structure of the recombinant PTX3 used in this study. (**B**) Images of liposomes (DMPC:40, Chol:50, DMPG:5, DGS-Ni-NTA:5, mol%) stained with uranyl formate and imaged via electron microscopy (EM) with and without PTX3. The panel with PTX3 (right) represents a tomographic slice of 0.45 nm thickness, whereas the panel without PTX3 (left) is a micrograph. (**C**) PTX3 visualised binding to liposomes via cryo-electron microscopy (cryoEM).*

Both panels represent tomographic slices 3.48 nm thick. Scale bars in each panel represent 100 nm. N-terminal domains are indicated with red arrows.

Enzyme-linked immunosorbent assay (ELISA) was used to reveal that PTX3 bound to purified C1, C1q (10 µg/ml) or C1 present in normal human serum (10%, NHS) compared to controls (**Fig. 3A**). To monitor if this binding resulted in complement activation, a proteolysis assay was used to measure the rate of C1 mediated cleavage of a self-quenching fluorescent peptide in the presence or absence of liposomes, PTX3 and purified C1. However, unlike the short pentraxin CRP (**Fig. 3B**), PTX3 did not appear to induce proteolytic activity in the C1 complex on liposomal surfaces (**Fig. 3C**). This could reflect the low concentration of PTX3 used when compared to CRP (500 vs 5000 nM), even though the concentration used is above that which has been detected in human serum(229, 230). However, PTX3 is locally produced at sites of inflammation where it could be present at much higher local concentrations(231-233) and could mean that higher concentrations of PTX3 are required to cause complement activation. Alternatively, the lack of complement activation could represent fluid phase inhibition of C1 by PTX3 as has been previously reported during the silent clearance of apoptotic cells(228, 234). To circumvent this, excess fluid phase PTX3 could be removed by separating it from lipid bound PTX3 via centrifugation, much as was done for the analysis of co-sedimented protein above (**Fig. 1**). Conversely, the use of recombinant tagged PTX3 could disrupt important interactions in the N-terminal domain that would otherwise lead to higher order multimer formation required for C1 activation(140). This has occurred for other systems where N-terminal interactions are crucial for higher order oligomer formation, such as COPII(235, 236), and it is known that the N-terminal of PTX3 is important in regulating the assembly of higher order structures during extracellular matrix organisation (237). Similarly, binding via an artificial tag could also prevent a conformational change required to activate PTX3, much as is hypothesised to be the case for CRP(107, 124) and occurs for IgM(9). To circumvent this in future studies, cleavage of the purification tags using TEV protease could be utilised, although the need for DTT for optimal TEV protease functioning could disrupt the quaternary structure of PTX3. Alternatively, a method to purify untagged PTX3 from cells could be used as has previously been reported(140), in conjunction with the use of a native membrane associated ligand.

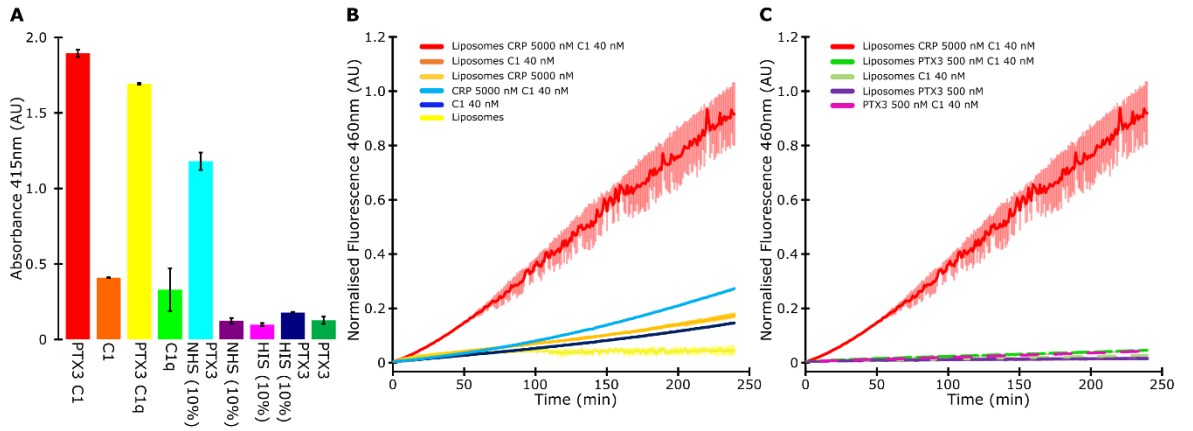

Figure 3: PTX3 binds to C1q but does not activate the protease domains C1r and C1s when bound to liposomes. *(**A**) Binding of immobilized PTX3 to purified C1 (10 µg/ml), C1q (10 µg/ml) or C1q in normal human serum (10%, NHS) as detected via enzyme-linked immunosorbent assay (ELISA) with an anti-C1q antibody. Heat inactivated serum (HIS) was used as a control. Errors bars represent the standard deviation of triplicate wells. The proteolytic*

*activity of the C1 domain was monitored by cleavage of a self-quenching fluorescent peptide. (**B**) CRP (5000 nM) stimulated the protease domains of the C1 complex in presence of liposomes (DMPC:80, LPC:20, mol%) and C1 (40 nM). (**C**) PTX3 (500 nM) does not stimulate the C1 complex in the presence of liposomes (DMPC:40, Chol:50, DMPG:5, DGS-Ni-NTA:5, mol%) and C1 (40 nM). The trace for liposomes in the presence of CRP and C1 is in both panels to allow comparison. Error bars represent the standard deviation between duplicate wells.*

Given the hypothesised limitations of the current experimental setup, we sought a native transmembrane PTX3 ligand. PTX3 is known to interact with several membrane associated ligands such as CD44(238), dectin-1 (CLEC7A)(19) and P-selectin(52), though the latter can be modulated via the N-linked glycan on PTX3, leading to variation between PTX3 from different sources. To find interactors that work specifically with the recombinant PTX3 used in this study, a genome-wide CRISPR-based screen of human transmembrane receptors was used to scan for possible binding partners(239). This revealed a clear binder, CLEC1B, which showed almost ten-fold greater association with PTX3 than the second highest hit in the screen, FCGR1B (**Fig. 4A**). This was validated via fluorescence-activated cell sorting (FACS) of PTX3 added to cells overexpressing CLEC1B from two separate gRNAs or cells with no CLEC1B expression using a control gRNA (**Fig. 4B**). This showed that PTX3 associated specifically to the CLEC1B expressing cells, suggesting a true interaction between PTX3 and CLEC1B (**Fig. 4B**). This illustrates that CLEC1B could be used in future studies as a native membrane ligand for PTX3 and possibly be used as a base to study complement activation with C1 added in tandem. In order to achieve this, liposomes decorated with CLEC1B could be prepared using methods previously applied to studying protein import(240) and could be expanded to include other ligands, such as CD44(238) and dectin-1 (CLEC7A)(19). Alternatively, a host of other ligands could be presented on lipid membranes using purification tags as used for PTX3 above, including FGF-2(41, 45, 46, 214, 241) and influenza hemagglutinin(51). This would avoid disrupting interactions between, or conformational changes within, PTX3 complexes, but still allow decoration of lipid membranes with PTX3 bound to biologically-relevant ligands.

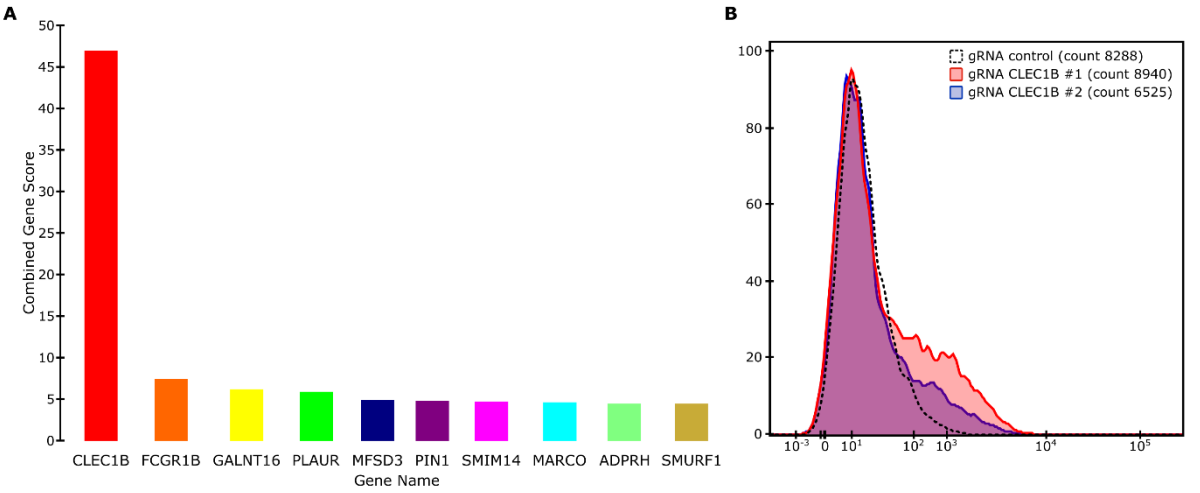

Figure 4: Identification of CLEC1B as a native transmembrane PTX3 ligand. *(**A**) A genome wide CRISPR screen for transmembrane interactors of PTX3 identified CLEC1B as a ligand (top 10 hits are shown). (**B**) Fluorescence-activated cell sorting (FACS) showing detection of PTX3 binding using control or CLEC1B guide RNAs (gRNAs) as detected via secondary antibodies conjugated to puromycin. Cell counts are shown in brackets.*

PTX3 has a different protein architecture when compared to the short pentraxins, including an additional flexible N-terminal region involved in binding to a range of ligands(36) (**Fig. 5A**). As PTX3 can bind to ligands at different parts of the protein complex, higher order oligomers

of PTX3 could exhibit different conformations consisting of different heights and geometries when binding to different ligands (**Fig. 5B&C**). This is particularly relevant in light of the recently published structural data of IgG3 bound to C1 and how the height of this complex has been postulated to lead to enhanced complement activation via decreased interference of the protease domains from the corona of deposited complement factors(138). Additionally, the fraction of the N-terminal domain that is available to participate in inter-PTX3 interactions would be different depending on the ligand that is bound. This could lead to different geometries of PTX3 multimers decorating the membrane when bound to different ligands (**Fig. 5C**). Although it is unknown how this would relate to complement activation or immune function, this hypothesis describes PTX3 as a multi-modal scaffolding complex, that induces different physiological outcomes depending on the biological context.

CryoET imaging of PTX3 bound to native membrane ligands would provide greater insight. Both CD44(238) and dectin-1 (CLEC7A)(19) are known membrane associated interactors with PTX3, with this study revealing a third, CLEC1B (**Fig. 4**). This could have particular relevance for cancer, as PTX3 interacting with both CD44 and CLEC1B has been highlighted as important (238, 242). Furthermore, the role of CLEC1B and dectin-1 in host defence against a diverse range of pathogens including fungi, HIV, and mycobacteria, may reveal crucial insights into the innate immune functions of PTX3(243). Furthermore, as CLEC1B can bind to both viruses and induce platelet aggregation, it would be intriguing to see if PTX3 could link these processes together. This could represent a link between clotting and viral infection mediated by the innate immune system, in a similar manner to that observed with SARS-CoV-2 infection(244). Moreover, PTX3 has been linked to the severity of SARS-CoV-2 infection by several groups(201, 245, 246), suggesting insights into PTX3 bound to viral ligands could help develop new therapies. To conclude, a membrane-based platform where PTX3 can be screened for interactions with ligands such as factor-H has been established. However, some limitations exist, such as the lack of higher order oligomer formation and complement activation. This could be circumvented with a more native linkage between PTX3 and liposome, via natural transmembrane ligands such as CD44, dectin-1 or CLEC1B, providing insight into a range of pathologies from cancer to viral infection.

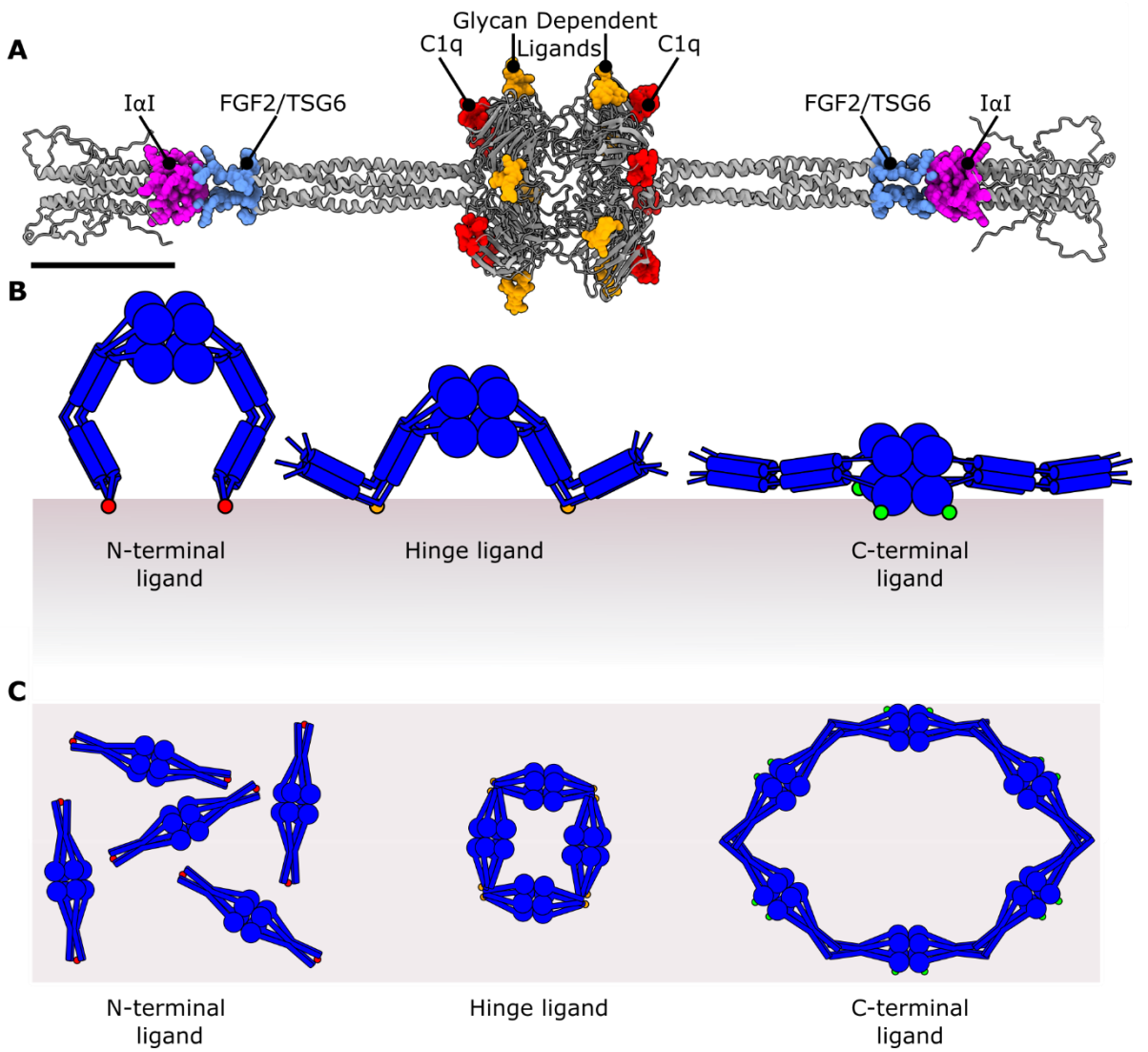

Figure 5: Multi-modal binding of PTX3. *(**A**) Ligand binding domains of PTX3 mapped onto the full atomic model (PDB-Dev: PDBDEV_00000141). (**B**) Different configurations of PTX3 binding to membranous ligands that bind to different parts of the protein complex. (**C**) Possible ramifications for multimer assembly on a surface if mediated via N-terminal regions. N-terminal ligands, e.g. Ni-NTA, would not lead to multimer formation.*

Methods

PTX3 expression and purification

A codon-optimised gene fragment containing a signal sequence, double strep tag, His_6-tag and TEV-tag with the following DNA sequence was ordered from GeneArt, with the HindIII (underlined) and BamHI (bold) restriction sites highlighted.

AACAAC<u>AAGCTT</u>GCCGCCACCATGGAATTTGGGCTGAGCTGGGTGTTCCTCGTCGCTTTGCTTAG
AGGCGTTCAGTGCTGGAGCCATCCTCAGTTCGAGAAGGGAGGGGGAAGTGGGGGAGGCTCAGGAG
GCAGCGCATGGTCTCACCCCCAGTTTGAAAAGGGTTCTGGCGGTTCCGGCCACCACCATCATCAC
CACGGGTCGGGCGGTTCCGGCGAGAACCTGTACTTCCAAGGAGAGAACAGCGACGACTACGACCT
TATGTACGTGAACCTGGACAACGAGATCGACAACGGACTGCACCCCACCGA**GGATCC**AACAAC

The gene was cloned into a pcDNA3.3 expression vector that contained a His_6-tagged version of PTX3 used previously(36), using HindIII and BamHI restriction sites flanking the gene fragment. Correct insertion was checked by Sanger sequencing at the Leiden Genome Technology Center. This produced the following PTX3 protein sequence preceded by a signal sequence (bold), double strep tag (italic), His_6-tag (italic) and TEV-tag (italic and bold). The inserted gene fragment is highlighted below (underlined).

MEFGLSWVFLVALLRGVQC*WSHPQFEK*GGGSGGGSGGSA*WSHPQFEK*GSG*HHHHHH*GSG***ENLYFQ***
GENSDDYDLMYVNLDNEIDNGLHPTEDPTPCACGQEHSEWDKLFIMLENSQMRERMLLQATDDVL
RGELQRLREELGRLAESLARPCAPGAPAEARLTSALDELLQATRDAGRRLARMEGAEAQRPEEAG
RALAAVLEELRQTRADLHAVQGWAARSWLPAGCETAILFPMRSKKIFGSVHPVRPMRLESFSACI
WVKATDVLNKTILFSYGTKRNPYEIQLYLSYQSIVFVVGGEENKLVAEAMVSLGRWTHLCGTWNS
EEGLTSLWVNGELAATTVEMATGHIVPEGGILQIGQEKNGCCVGGGFDETLAFSGRLTGFNIWDS
VLSNEEIRETGGAESCHIRGNIVGWGVTEIQPHGGAQYVS

PTX3 protein was produced by transfecting 25 µg plasmid DNA into Expi293F™ cells in Expi293™ Expression Medium using Opti-MEM and the ExpiFectamine™ 293 Transfection Kit (all ThermoFisher, USA) according the manufacturer's instructions. Supernatant containing PTX3 was harvested 5-7 days post-transfection, centrifuged to remove cellular debris and filtered sequentially through 0.45 µm and 0.2 µm filters (Cytiva, USA).

All steps for protein purification were performed at 4°C unless otherwise stated. Cellular supernatant was dialysed in 12 kDa molecular weight cut-off dialysis tubing (Sigma-Aldrich, USA) against into Tris-HCl 20 mM, NaCl 500 mM, pH 8.0 (buffer A) for four hours and then overnight at in 2 L and 5 L of buffer, respectively. Next, the dialysed supernatant was supplemented with 16 mM imidazole, then added to 10 ml of Ni-NTA beads (ThermoFisher, USA) and incubated overnight on a rotor. This was then added to a gravity flow column and washed with 10 column volumes of buffer A with 30 mM, 50 mM and 70 mM of imidazole, respectively. The protein was eluted with buffer A containing 100 mM, 250 mM and 500 mM imidazole. Fractions were analysed using SDS-PAGE and those containing PTX3 were dialysed overnight against 3 L of Tris buffered saline (TBS; Tris-HCl 50 mM, NaCl 150 mM, pH 7.4). Subsequently, the protein was further purified using SEC with an S200 column (24 ml bed volume, Cytiva, USA). Fractions were analysed using SDS-PAGE and Western Blot, as well as their ability to activate complement via ELISA. Quality control was carried out on a S200 increase SEC column (2.4 ml bed volume, Cytiva, USA).

Liposome production

Liposomes were prepared using dimyristoylphosphatidylcholine (DMPC), dimyristoylphosphatidylglycerol (DMPG), cholesterol and 1,2-dioleoyl-sn-glycero-3-Ni-NTA (DSG-Ni-NTA) purchased from Avanti Polar Lipids (USA). Lipid films were composed of DMPC–DMPG–cholesterol–DSG-Ni-NTA (40 : 5 : 50 : 5 mol%). Components were dissolved in chloroform–methanol (9 : 1 v/v) before drying under nitrogen gas and desiccation overnight. Films were rehydrated at 60°C for 1 hour in TBS to a final lipid concentration of 0·8 mg/ml. Lipid films were then pipetted off the sides of the glass vials and vortexed for 10 seconds.

Liposomes were then extruded through a 400 and 100 nm membrane sequentially with 11 passes each, using an extruder from Avanti Polar Lipids (USA). For CRP binding the same protocol was followed but with liposomes prepared using DMPC and 1-myristoyl-2-hydroxy-sn-glycero-3-phosphocholine (LPC, Avanti Polar Lipids, USA) at a ratio of 80 : 20 (mol%).

Liposome binding

Liposomes (50 µl per reaction) were incubated with PTX3 (500 nM) overnight at 4°C before being mixed with ice-cold NHS (10%) and made up to 70 µl with TBS. This was incubated on ice for 30 minutes before being spun down at 21,460 g and 4°C for 15 minutes. Next, the supernatant was discarded and the pellet resuspended in 70 µl TBS. Subsequently, the sample was spun as before and the pellet resuspended in 20 µl µl TBS, which was then used for further analysis. For controls PTX3, liposomes or NHS were replaced by ice told TBS.

SDS-PAGE

Sample were diluted in 2× Laemmli buffer (65.8 mM Tris-HCl, 26.3% (w/v) glycerol, 2.1% SDS, 0.01% bromophenol blue, pH 6.8) with DTT (50 mM) and heated to 99°C for 10 mins, briefly centrifuged at 700 g, and then loaded onto onto a 4-12% pre-cast Bis-Tris Protein Gels (Bolt™, Invitrogen™, Thermo Fischer scientific, USA) and run at room temperature for 35 minutes at 200 V. Gels were stained with SimplyBlue™ to visualise protein content (Thermofisher, USA).

Western Blot

For Western Blotting, samples were separated using PAGE as described above. Samples were transferred to nitrocellulose membranes in Tris-Glycine buffer (Tris 12 mM, Glycine 96 mM) with 10% methanol. The membranes were then blocked using phosphate buffered saline (PBS) with 0.1% Tween 20 and 5% milk (blocking buffer). After washing three times with blocking buffer, proteins were detected with an anti-His_6 primary antibody (Thermofisher, USA) diluted 1:1000 at 4°C overnight. The membranes were then washed as before, and subsequently a HRP linked goat anti-mouse antibody (Dako, Denmark) diluted 1:1000 was added and incubated with the membranes at room temperature for 30 minutes. The membranes were washed twice in blocking buffer and four times in PBS with 0.1% Tween 20. Detection was performed with ECL™ reagent and imaged on a ChemiDoc™ gel imaging system (Thermofisher, USA).

Negative stain

First, PTX3 was incubated with liposomes at a ratio of 1 µg of protein per 1 µl of liposomes overnight at 4°C. These mixtures were then added to precooled Vivaspin™ spin filters (Sartorius, Germany) with a 1000 kDa cut off and made up to 500 µl with ice-cold TBS, before spinning at 14,000 g at 4°C for 5 minutes. Flow through was discarded and the spin filter was topped up with 500 µl ice-cold TBS. This was repeated two more times. Next, 6 µl of the dead volume from the spin filter was applied to continuous-carbon EM grids (200 mesh EM grids, Electron Microscopy Sciences, USA) and incubated for 5 minutes. Excess liquid was then removed with filter paper (Whatman, Merck, USA) and 10 µl of uranyl formate (2%) was added to stain for 10 seconds, before excess stain was removed with filter paper. Samples were left to air-dry before being imaged on an FEI Tecnai 12 Twin Transmission electron

microscope (ThermoFisher, USA) with a LaB_6 filament operating at 120 kV. Tilts series were acquired with a defocus of ~4 µm on an Eagle 4k x 4K CCD camera (ThermoFisher, USA), at a magnification of ×49000 using a discontinuous tilt scheme from -50° to 50° in 4° increments. Tomograms were reconstructed in IMOD using patch clamp tracking and subsequent weighted back projections with a SIRT like filter.

CryoEM

Liposomes were incubated with PTX3 overnight as described above before ice-cold protein A albumin-coated 10 nm gold colloids were added. Freshly plasma-cleaned 200 mesh copper grids, with lacey-carbon support (Electron Microscopy Sciences, USA), were loaded into a Leica EMGP (Leica Microsystems, Germany) and 6 µl sample was applied to the grids. Samples were incubated for 60 sec on the grid in the chamber at 4 °C and 65% humidity. The grids were blotted for 1.5 sec from the back and vitrified in liquid ethane. Grids were clipped and stored in liquid nitrogen until usage.

For tilt series acquisition, a Talos Arctica (ThermoFisher, USA) operating at 200 kV with a K3 direct electron detector and a Bioquantum energy filter (Gatan, USA) was used. The energy filter was set to a slit width of 20 eV. Tilt series were acquired using Tomo 5.5.0 (ThermoFisher, USA) in counting mode at 49,000× magnification with a pixel size of 1.74 Å using a dose-symmetric scheme from 0 to +/- 57 °, in 3 ° increments in a dose-symmetric tilt scheme. Focusing between -4 µm to -6 µm and tracking were performed before each tilt acquisition. A total dose of 60 e-/Å2 was used.

Before reconstruction, raw frames were aligned using the “alignframes” command from IMOD 4.11 54. Tomograms were reconstructed after 2× binning of tilt series using IMOD 4.11 with weighted back projections with a SIRT like filter equivalent to five iterations.

Enzyme-linked immunosorbent assay (ELISA)

ELISAs were performed using 96 well microtiter plates coated with 50 µl of PTX3 at 10 µg/ml in 0.1 M sodium carbonate (pH 9.3). For coating controls, only the sodium carbonate solution was added. These were incubated for one hour at 37°C, then washed three times in phosphate buffered saline (PBS) with 0.05% Tween 20. Subsequently, wells were blocked with 100 µl of 0.1 M spermidine, before being incubated and washed as previously described. Next, 50 µl of purified C1 (10 µg/ml, Complement Technology, USA) or C1q (10 µg/ml, Complement Technology, USA) diluted in TBS, or NHS (10%, Complement Technology, USA) or HIS (10%, NHS heated at 56°C for 30 minutes) diluted in RPMI (Thermofisher, USA), were incubated for one hour at 37°C before washing. To detect C1, 50 µl of a rabbit polyclonal anti-human C1q (Dako, Denmark) diluted 1:1000 was added and incubated for one hour before being washed as described above. Thereafter, 50 µl of a goat anti-rabbit conjugated to HRP diluted 1:5000 (Dako, Denmark) was added, then incubated for one hour and washed. Absorbance at 415 nm was measured 60 minutes after addition of 50 µl of 2.5 mg/ml 2,2'-azino-bis(3-ethylbenzothiazoline-6-sulfonic acid) (ABTS) in citric acid buffer (0.15 M, pH 4.2) with 0.015%

(v/v) H_2O_2 using a Clariostar plus plate reader (BMG Labtech, Germany). Error bars represent standard deviation of triplicate wells.

C1 protease activity assay

All steps were done at 4° C until measurements were started with liposomes added at half the total reaction volume. For PTX3, 500 nM was added to liposomes composed of DMPC–DMPG–cholesterol–DSG-Ni-NTA (40 : 5 : 50 : 5 mol%) in TBS with 500 µM $CaCl_2$. For CRP, 5000 nM was added to liposomes composed of DMPC-Lysophosphatidylcholine (DMPC-LPC, 80 : 20 mol%) in TBS with 5 mM $CaCl_2$. Next, a fluorescent peptide substrate, Boc-Leu-Gly-Arg-Amino Methyl Cumarin (LGR-AMC, PeptaNova GmbH, Germany), dissolved in DMSO (5% DMSO final concentration) was added at 500 µM, before buffer exchanged purified C1 complex in TBS with 500 µM $CaCl_2$ (Complement Technology, USA) was added to the reaction (40 nM). Subsequently, proteolytic activity of purified C1 complex was measured in real time via cleavage of LGR-AMC on a Clariostar plus plate reader (BMG Labtech, Germany). Measurements were taken every minute for a period of four hours at room temperature, with excitation and emission set at 360 and 460 nm respectfully. The first measurement of each condition was subtracted as background, before normalizing the entire plate to the highest value. Duplicate wells were then averaged and the standard deviation between them was calculated and represented as error bars.

Genome scale CRISPR screening

For CRISPRa screening for transmembrane interactors of PTX3, K562 cells were transduced with dCAS9-Blast, a kind gift from Feng Zhang (Addgene #61425), and the genome-wide Calabrese activation library (sublibrary A+B), a kind gift from John Doench (Addgene #1000000111). Transduced cells were selected using blasticidin (5µg/ml) and puromycin (2µg/ml) and after seven days, two batches of 50million cells were stained with His_6-PTX3. Cells that labelled positive for PTX3 (between 0.01 and 0.1%) via detection with a mouse anti-His_6 antibody (Thermofisher, USA), were sorted and genomic DNA was isolated from these cells, as well as from the unsorted cells. gDNAs were amplified as above and sequenced using the Ilumina NovaSeq6000. Inserts were mapped to the reference and analysis of gRNA enrichment was done using PinAPL-Py.

Transfections and transductions

For the generation of CLEC1B -expressing cells, virus was produced as described above for the CRISPR screens. To generate gRNA-mediated CLEC1B overexpressing cells, K562 cells were first stably transduced with the lenti dCas-VP64 vector (Addgene plasmid # 61425) and selected using blasticidin (10ug/ml). These cells were subsequently transduced with the pXPR_502 vector (Addgene plasmid # 96923) containing a gRNA sequence targeting CLEC1B, and selected using puromycin. The guide sequences used were: CLEC1B sgRNA #1: 5'-TGATCTTCCTGTCTTTAGTA-3'. Clec1b sgRNA #2: 5'-CAAATGTGTCCCATCTCACA-3'. All oligo sequences used in this study were obtained from Integrated DNA technologies. Cells were sorted as described above.

Acknowledgements: This research was supported by the following grants to THS: European Research Council Grant 759517; The Netherlands Organization for Scientific Research Grants OCENW.KLEIN.291 and VI.Vidi.193.014.

Author Contributions: Tom A. W. Schoufour and Ruud H. Wijdeven performed the genome wide screen and FACS validation with guidance from Jacques Neefjes. Douwe J. Dijkstra and Teun T. van der Klugt and Trouw cloned and expressed recombinant PTX3. Dylan P. Noone performed protein purification, sedimentation assays, SDS-PAGE, Western Blot, liposome production, EM, cryoEM, ELISA and protease assays. Dylan P. Noone also analysed data and wrote the manuscript, with input and guidance from Thomas H. Sharp.